Invasion Percolation in Presence of Gravity

Ma'soum, Sara•; Masihi, Mohsen*+

Faculty of Chemical and Petroleum Engineering, Sharif University of Technology,
P.O. Box 11365-9465 Tehran, I.R. IRAN

ABSTRACT: *Simultaneous capillary dominated displacement of the wetting and non-wetting phases are processes of interest in many disciplines including modeling of the penetration of polluting liquids in hydrology or the secondary migration in petroleum reservoir engineering. Percolation models and in particular invasion percolation is well suited to characterize the slow immiscible displacement of two fluids when both the gravity and viscous effects are negligible. In particular, the characteristic of the percolating cluster and the other important percolation properties at the breakthrough can be inferred. However, with the inclusion of the gravity forces, the behavior may change. For example, as the magnitudes of the gravity forces are comparable to the capillary forces, we have observed a transition in the structure of the interface (i.e. invasion front) depending on the dimensionless Bond number (i.e. ratio of gravity to capillary forces). We have taken a numerical study of the displacement of two immiscible fluids in the presence of the gravity force in a network of random pores. The main contribution is to investigate the effect of heterogeneity by considering various throat size distributions. We consider the injection to take place from one side of the system and displace the displaced fluid from the other side. The condition of the stability or instability of the front (or interface) is observed to be dependent on the dimensionless bond number as well as the heterogeneity of the system.*

KEY WORDS: *Pore scale, Modelling, Immiscible displacement, Invasion percolation, Gravity.*

INTRODUCTION

Flows of fluids through porous media is important in many industrial and geological applications, such as in studying of the efficient hydrocarbon recovery techniques by reservoir engineers or in modelling ground water flow by hydrologists [1]. The porous media which are typically made of rock grains and disordered void spaces are usually characterized by porosity ϕ and permeability k

in the case of a single phase flow. The pore spaces are approximately 10-100 μm across and are usually occupied by hydrocarbons and water in a typical hydrocarbon reservoir. Hence we usually observe a multi phase flow in porous media. Fluid displacement in porous media depending on the scale of the region can be controlled by several forces including the pore scale capillary forces

71

(on the pore level), viscous forces and gravity forces (over larger distances) [2]. Hence, the type of the displacement observed, depends on the capillary number, the ratio of the viscous pressure drop at the pore scale to the capillary pressure, and the Bond number, the ratio of the hydrostatic pressure drop over a pore to the capillary pressure. Typical flow rates in reservoirs are of order of a few feet per day. It should be noticed that the full description of displacement process in porous media is very difficult due to the variety of physical phenomena involved. For example, the flow of two immiscible fluids depends on the wetting properties of the two fluids, their viscosity ratio, their respective densities, and displacement rate. Moreover, the experimental measurements are extremely difficult to perform and at low saturations the results are very uncertain. This is why numerical simulations usually rely on the available empirical correlations to predict the relative permeability and capillary pressure from the measured two-phase properties. However, it is important to have a reliable physically-based tool that can provide plausible estimates of these macroscopic properties. *Fatt* [3] initiated describing the pore space as a network of pores connected by throats with some idealized geometry to find the capillary pressure and relative permeability curves. Since then, the capabilities of network models have improved enormously and have been applied to describe many different processes. *Blunt & King* [4] derived some macroscopic parameters from simulations of pore scale flow through simple networks. For a random close packing of spheres, *Bryant & Blunt* [5] were able to predict elastic and electrical properties and relative permeability of the network. *Øren et al.* [6] extended this approach by reconstructing a variety of sandstones and generating topologically equivalent networks from them. Using network-based models several authors have been able to predict the macroscopic flow properties and oil recovery for a variety of two and three phase systems [7].

Darcy's law is the basic transport equation at the continuum scale for a typical two phase system where the k_{ri} are the relative permeabilities of each phase, dependent on the fluid saturations (S_i).

$$u_i = -\frac{Kk_{ri}(S_i)}{\eta_i}\nabla P_i \qquad (1)$$

This law is used in conjunction with the assumption of incompressible fluid for the total flux to give an equation for the continuity of each phase as follows:

$$\phi\frac{\partial S_i}{\partial t} + u_i\nabla S_i = 0 \qquad (2)$$

This produces the most basic set of equations used to describe multi-phase flow in porous media. In practical application of this, there is question of how to find the efficient microscopic averaging of the pore scale physics in order to determine the critical parameters such as relative permeability. One physically based approach to do this is to use percolation concepts from percolation theory.

The mathematical description of percolation theory was first introduced by *Broadbent & Hammersley* [8]. The spread of a fluid through a disordered medium may happen in two ways. In the first type the fluid particles decide were to go in the randomness medium which is the familiar diffusion process. In the other type the randomness is ascribed to the medium and that is the medium which dictate the path of particles. This approach that is called percolation process was considered by *Broadbent & Hammersley*. A description of this mathematical theory was given by Stauffer and *Aharony* [9] and various applications of this theory can be found in *Sahimi* [10]. There is another kind of percolation called invasion percolation that was first described by *Wilkinson & Willemsen* [11]. The model is motivated by the problem of one fluid displacing another from a porous medium under the action of capillary forces, but in principle it may be applied to any kind of invasion process which proceeds along a path of least resistance. This type of percolation model has been used to either validate the experimental observations at the pore scale or to infer macroscopic properties of the pore networks. Many experiments using micro models have been performed to study either displacement mechanisms at the pore level or displacement and trapping at the large scale for considering the effect of capillary, gravity and viscosity forces [12, 13]. For example, *Toubou et al.* [12] found a good agreement between simulated patterns of the stochastically generated pore network (such as trapping and fingering) and the micro-model based experimental observations.

PERCOLATION CONCEPTS

Percolation theory is the mathematical model of the connectivity in a geologically complex system [9].

It has applications in many areas from the spread of diseases to the conductivity of porous media used for hydrocarbon recovery. Consider an infinite lattice of sites which are placed randomly and occupied with a probability p. Clusters from the occupied neighbouring sites and grow in size as the occupancy probability increases. There is a particular value of p, called the percolation threshold p_c^∞, at which one large cluster spans the whole region. There are also other small clusters which get absorbed to the largest cluster as p further increases. Then, there are some simple scaling laws which describe the behaviour of the system around the threshold p_c^∞. These are:

$$P(p) \propto \left(p - p_c^\infty\right)^\beta \qquad (3)$$

$$\xi(p) \propto (p - p_c^\infty)^{-\nu} \qquad (4)$$

Where P(p) is the probability that an occupied site belongs to the spanning cluster (i.e. connected fraction which represents the strength of the percolating cluster) and ξ(p) is the correlation length (which is a measure of the "typical" size of the clusters, excluding the infinite cluster when the system is above the threshold). Note that the correlation length ξ(p) is related to the two point correlation function g®, which is the probability of two sites, separated by a distance r, being in the same cluster. The important feature is that the critical exponents β and ν is independent of the kind of the lattice or even if there is a lattice or not (continuum system); they only depend on the dimensionality of space (i.e. 2D or 3D). Values for β=5/36 and 0.4 (in two and three dimensions respectively), and ν=4/3 and 0.88. This is known as universality and is an important concept in percolation theory which enables us to study and understand behaviour of a very wide range of systems without needing to worry too much about the small scale details. However, the percolation threshold does depend on the detail of the lattice and has to be determined from few simulation results [9]. The other issue we often face is due to the finite size effects as all systems are finite in size. This is addressed using the known finite size scaling within percolation theory [9]. Recently, the effect of anisotropy and size distribution on the percolation properties of finite size systems in the case of fractured porous medium has been addressed [14].

PERCOLATION MODEL OF THE IMMISCIBLE DISPLACEMENT

Let us start with a simple case of displacement of a fluid by another fluid in a two-phase system i.e. the problem of oil/water flooding or secondary migration. Fluid movement can be governed by viscous, gravity and capillary forces [15]. For systems without gravity we expect different flow regimes depending on the capillary number. Viscous forces are mainly dependent on the viscosity of the fluids. The high viscosity of the displaced fluid can lead to a highly unstable displacement pattern with a rapid breakthrough of the displacing fluid into the displaced fluid called viscous fingering [16]. This can be neglected by considering the situation that the displacing fluid has a higher viscosity than the displaced fluid. Then, for slow displacements the invasion percolation, a specific form of percolation theory, can be used to model the displacement and to describe the structure and amounts of fluids in a two-phase displacement at breakthrough [11, 17]. The displacement in the model is controlled by the heterogeneity of the capillary pressures along the interface.

Consider a lattice with sites and bonds representing pores and throats respectively. The throats can be classified into allowed, occupied and accessible and two processes can be considered for an immiscible displacement. An event where a wetting phase (i.e. water) is displaced by a non-wetting phase (i.e. oil) with a positive capillary pressure is called drainage while imbibition is a process where the water enters the porous medium and displaces the oil phase. This simple network model along with percolation concepts can then be used to find many important properties such as capillary pressure and/or relative permeability curves in porous media [18, 19]. First consider the invasion percolation for modelling of a drainage process. In order to overcome the pressure caused by the interfacial pressure to drive the oil into the water phase we need to apply an equivalent to capillary pressure P_c as follows:

$$P_c = P_{nw} - P_w = \frac{(2\sigma\cos\theta)}{r} \qquad (5)$$

Where σ is the interfacial tension, θ is the contact angle and *r* is the pore throat radius.

In this study we have used a network of pores linked by throats of varying radii. The experimental observations of rock permeability data show a skewed distribution
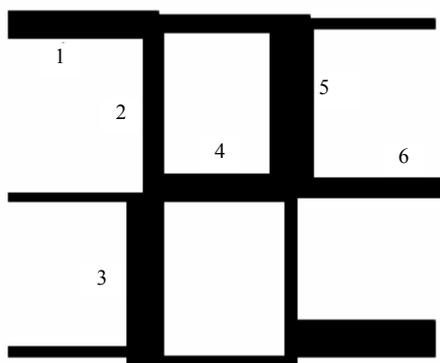
73

Fig.1: A simple illustrative network of pores linked by the throats of varying radii. The numbers represent the filling order of pores.

Fig. 2: A typical percolation structure at the breakthrough obtained from invasion percolation which simulates a drainage process.

with a long tail that often can be fitted with a log normal distribution. To model this we may use a log-normal distribution for the throat radii. Therefore in this simulation work in order to have a realistic permeability distribution, we used a lognormal distribution for the throat radii.

By increasing the pressure applied to the invading oil phase in the drainage process, the pores will first fill from the largest radius (where the entry pressure to fill is the lowest according to Eq. (5)). However, the pores can be filled only if they are connected to the inlet face and in contact with the oil phase. For example, in the simple illustrative network below where the oil comes from the left the pores will fill in the order 1, 2, and 3 and so on where the labels are in order of the throat radius.

By continuing this process, we get a percolating cluster with large regions unswept at the breakthrough of the oil to the right side of the system. The flow can only take place through sites already connected to the inlet. This is the simple model of invasion percolation as first introduced by *Wilkinson & Willemsen* [11].

We developed a programme in "MATLAB R2006a" to simulate this process and determine the required results. In practice, with this approach we do not need to solve the governing flow equations (Eq. (2)) since we model the displacement by considering the heterogeneity of the capillary pressures along the interface. In the standard invasion percolation model, the sites on a regular lattice are assigned random numbers to represent the capillary pressures (invasion thresholds) that must be overcome to invade them. The random numbers are taken from the pore throat radii distribution that is observed
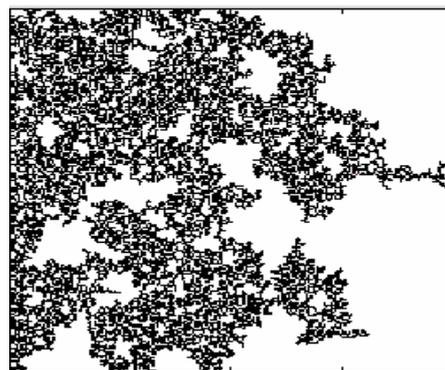
from CT-scan analysis on the rock sample. However, such analysis may be very difficult in the case of carbonate rock samples as the large scale heterogeneities is likely to be observed. Another complexity is the choice of triangular or circular geometry for the pore throat flow area. For simplicity we consider a two dimensional lattice of sites and neglect the effect of the pore throat flow area geometry. We assumed random numbers representing the resistance to the flow to be taken from a log normal distribution to be in line with the experimental permeability observations. However, again for simplicity reason and without lose of generality we may consider this to be in the range of (0, 1). On a lattice of size 200×200, we proceed the process by selecting the unoccupied external perimeter site with the lowest random number and filling it to represent the invasion of the non-wetting fluid into the widest pore throat. The unoccupied external perimeter consists of all the unoccupied sites with occupied nearest neighbor sites that can be reached by the random walk that originate outside of the region occupied by the growing pattern (i.e. cluster of occupied sites) and consist only those between unoccupied nearest neighbor sites. Fig. 2 represents a typical structure of invader fluid observed in the lattice of size200×200.

The main quantities of interest are the fraction of sites which become occupied by the oil, and the distribution of random numbers of those sites. In this simple model assuming no trapping, it is observed that the number of sites occupied by the invader in spanning cluster N_I may be scaled as $N_I \propto L^d$ where L is the lattice size and "d" is known as the fractal dimension of the cluster with

74

d = 1.89 and 2.52 in two and three dimensions, respectively. Notice that the values are consistent with the fractal dimensions of ordinary percolation theory. Moreover, the volume fraction of the invader S_I follows the scaling law $S_I \propto L^{-\alpha}$ where the numerical value for the exponent is α = 0.11 and 0.48 in two and three dimensions [11] that are consistent with a universal values derived from random percolation models. Hence, it has the same universality class as random percolation. Invasion percolation with trapping, on the other hand, causes the phenomenon known as residual oil. Numerical investigations have shown that the fractal dimension of the invader cluster is 1.82 in two dimensions which is less than 91/48 of random percolation with no significant difference in three dimensions. Moreover, the fraction of volume occupied by the invader is proportional to the grid size to power -0.18 in two dimensions. If we pursue with the invasion process beyond the point of percolation, a second percolation threshold is reached when the defender consists of isolated clusters only and the process stops. Then the system has reached saturation of residual oil. It should be noticed that although the properties of invasion percolation are consistent with that of random percolation the spanning clusters are not precisely the same.

INVASION PERCOLATION IN THE PRESENCE OF GRAVITY

In some situations the gravity forces acting on the density difference between the two fluids can be comparable to the capillary forces. In these cases we expect this to modify the local dominant forces depending on the scale of the study. Here we again model the slow flow displacement (by neglecting the viscous forces) on the same network as before but considering the gravity forces. We have examined how gravity forces can destabilize the interface, depending on the relative position of the denser fluid. Simulation results of slow displacement under gravity have shown that the interface keeps a finite width (defined as the root mean square value of the front extension in the direction of the flow) along the direction of apparent gravity in line with the experimental results of *Wilkinson* [2]. This width is found to scale with the Bond number where the numerical value of the scaling parameter is consistent with the gradient percolation prediction. The competition between gravitational and capillary forces can be described

in terms of the dimensionless Bond number B_o (the pore scale ratio between the effects of gravity acting on the density difference and the capillary forces) given by:

$$B_o = \frac{(\Delta\rho g \varepsilon)}{(\sigma / \varepsilon)} \qquad \Rightarrow \qquad B_o = \frac{\Delta\rho g \varepsilon^2}{\sigma} \qquad (6)$$

Where $\Delta\rho$ is the density difference between the two fluids, g is the acceleration due to gravity, ε is the pore or grain characteristic size and σ is the interfacial tension [20].

In order to carry out a systematic experimental study of the relationships between the invasion pattern and the Bond number, it is necessary to vary the interfacial tension, the density difference or the acceleration. σ and $\Delta\rho$ can be changed only by using a series of liquids. Since σ and $\Delta\rho$ cannot be varied independently, these quantities must be carefully measured for each pair of liquids. The acceleration g can be varied using a centrifuge. However, it is much more convenient to vary the effective acceleration due to gravity by using inclined surface. This was previously seen experimentally by using the porous medium consisting of a monolayer of glass beads trapped between two parallel sheets of transparent material [20]. The effective acceleration was varied by changing the angle of inclination. However, in reservoir conditions with a typical pore size of 0.1mm in sandstone reservoirs; for a gas injection the typical values of $\Delta\rho$=800 kg/m^3, σ=0.004 N/m, and for a water injection $\Delta\rho$=200 kg/m^3, σ=0.035 N/m may be used to estimate the bond number in the range of 0.0002-0.02.

The growth of the fluid-fluid displacement pattern can be described in terms of the propagation of growth front, or active zone, into the porous medium. In the first case the active zone was seen to be stabilized by the effects of gravity acting on the density difference between the two fluids. In such cases, the fluid-fluid displacement pattern can be described in terms of a compact packing of blobs of size ζ, and each blob has a self-similar fractal invasion percolation structure on scales in the range $\varepsilon < l < \zeta$. Similarly, the external perimeter of the fluid-fluid displacement pattern can be described in terms of a horizontal packing of blobs with self-similar fractal structure. Hence the active zone is the entire external perimeter as shown in Fig. 3. In the second case, the active zone was seen to be destabilized by the effects of gravity acting on the density difference between the two fluids, and a finger of the low density non-wetting fluid
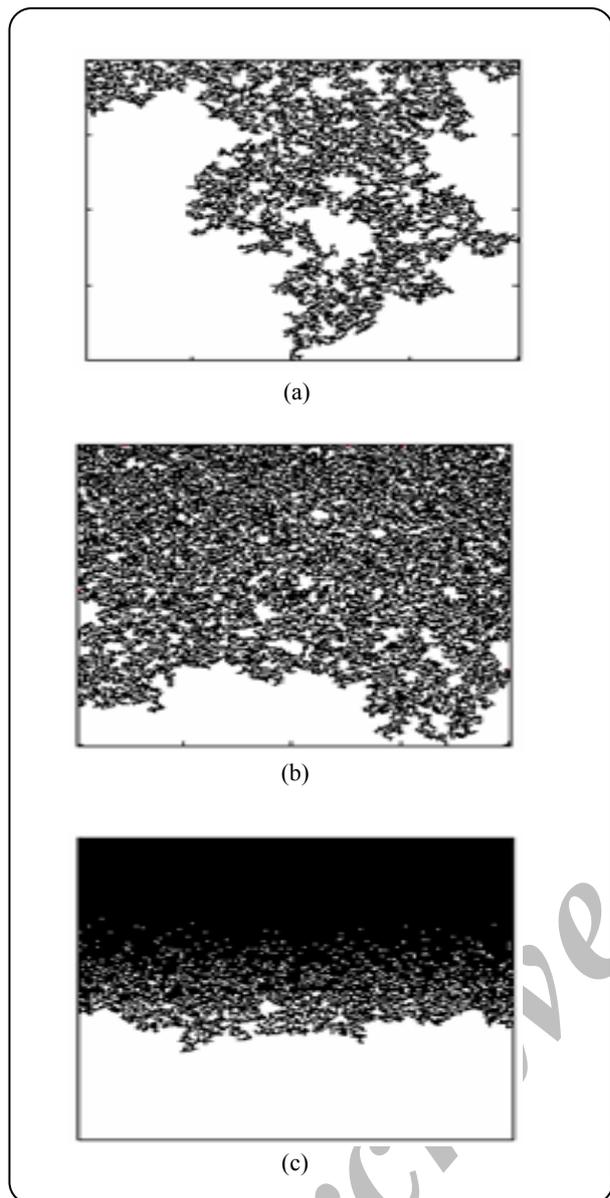
Fig. 3: Three realizations generated by the slow gravity stabilized displacement of a wetting fluid by a non wetting fluid in a quasi-two-dimensional porous medium in a lattice of size 200×200 *where (a) B=0, (b) B=0.0001, (c) B=0.001.*

was driven upwards through the porous medium. In such case, the fluid-fluid displacement pattern can be described in terms of a row of fractal blobs along the lower edge of the cell and a vertically oriented string of blobs that form a self-affine directed random walk. Again, each blob has a size of ζ and each blob has a fractal invasion percolation structure on scales in the range $\varepsilon < l < \zeta$: Hence, the active zone is confined to the last (highest) blob in the string of blobs as shown in Fig. 4.

The results of such experiments can be simulated quite well by using simple modifications of the standard site invasion percolation model. To do so the effects of gravity acting on the density difference between the two fluids can be represented by replacing the previous random numbers or invasion thresholds as follow [20]:

$$P = P_c(i) + BY(i) \tag{7}$$

Where $Y(i)$ is the y-coordinate of the ith site and B is the gradient acting in the y-direction which is related to the bond number. In the case of stabilized invasion percolation $B>0$, for example in the downward displacement at capillary control of a heavier fluid by the injection of a lighter fluid, or in drainage in a field of decreasing permeability, the percolation probability decreases in the direction of displacement, the effect of the gradient B is to prevent the trailing edges of the active zone from getting too far behind the leading edges. The crossover length ζ provides a measure of the width of the active zone. In the absence of a gradient, the external perimeter of an invasion percolation cluster is the same as the external perimeter of an ordinary percolation cluster. Figs. 3 and 4 represent the stabilized and unstabilized effect of the gravity [20, 21]:

In ordinary percolation, the correlation length, or crossover length is given by:

$$\xi \sim \left[\frac{(p-p_c)}{p_c} \right]^{-\nu} \qquad \text{for } p > p_c \tag{8}$$

Where p and p_c are respectively the occupancy probability and the percolation threshold and ν is the correlation length exponent. It is derived based on the fact that at the threshold point the typical size of clusters are comparable to the system size.

The exponent ν has a universal value of 4/3 for two-dimensional percolation problems. In gradient stabilized invasion percolation, the trailing edge of the active zone propagates by invading sites with thresholds that would be too large to occupy without the effect of the gradient. This corresponds to a percolation process in which the fraction of sites occupied exceeds p_c by an amount given by:
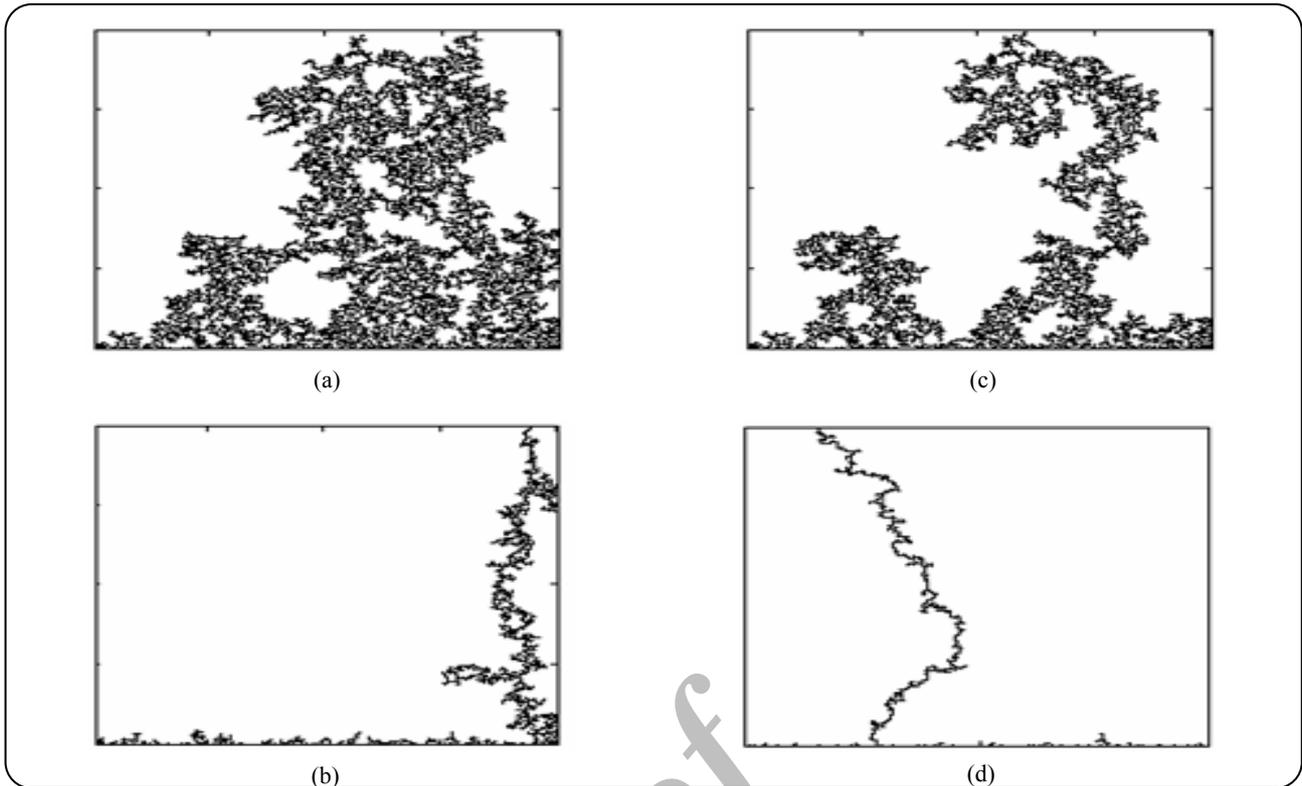
$$p - p_c \sim B\zeta \tag{9}$$

76

Fig. 4: Four realizations generated by the slow gravity destabilized displacement of a wetting fluid by a non wetting fluid in a quasi-two-dimensional porous medium in a lattice of size 200×200 where (a) B=0, (b) B=-0.0001, (c) B=-0.001, (d) B=-0.01.

It follows from Eqs. (8) and (9) that:

$$\zeta \sim (B\zeta)^{-\nu} \qquad \rightarrow \qquad \zeta \sim B^{-(\frac{\nu}{\nu+1})} \sim B^{-(4/7)} \qquad (10)$$

A similar argument can be used for gradient destabilized invasion percolation processes like the situation shown in Fig. 4. In this case, where B < 0, like the downward displacement at capillary control of a lighter fluid by the injection of a heavier fluid, the upward displacement of a heavier fluid by the injection of a lighter fluid, as in air sparging, or drainage in a field of increasing permeability, the gradient prevents the sides of the finger from propagating too far and broadening the finger too much. In ordinary percolation, the correlation length (or crossover length, ζ) provides a measure for the size of the largest clusters,

$$\xi \sim \left[\frac{|p - p_c|}{p_c} \right]^{-\nu} \quad \text{for } p < p_c \qquad (11)$$

Consequently, Eq. (10) also applies to gradient destabilized invasion percolation, and ζ is the size of the blob at the end of the finger, which corresponds to a finite cluster below the percolation threshold [20, 21].

When the displacement is unstable, and an increase of the Bond number enhances the instability it reduces the lateral width of the cluster ζ. For length scale smaller that ζ, the internal structure of the blobs is fractal, with a fractal dimensionality d = 1.82 in two dimension. Thus, the cluster mass distribution verifies the relationship,

$$M \approx \zeta^d \qquad (12)$$

And the number of occupied sites by the invading fluid scales as

$$N \approx \zeta^d (L/\zeta) \qquad (13)$$

Then, at the scale of the whole network, the saturation of the invading fluid can be written as:

$$S_o \sim \frac{N}{L^2} \qquad \rightarrow \qquad S_o \sim (\frac{1}{L})(B^{-\gamma}) \qquad (14)$$

where $\gamma = \dfrac{(d-1)\nu}{\nu+1}$

77

For two dimensional lattices the numerical value for the exponent is $\gamma \approx 0.47$ [20].

We measure numerically the width of the finger cluster and saturation with respect to the bond number by simulation of 10 samples and draw the curve on a log-log scale which is shown in Figs. 5 and 6. From these figures we found the slops corresponding to width of the finger cluster and saturation are respectively-0.58 and -0.44 which are consistent with theoretical predictions.

As can be seen in Figs. 5 and 6 at high bond numbers the gravity force is dominant and both the width of the finger cluster and the saturation decreases significantly (see fig. 4). The implication on secondary migration, for example, is that the magnitude of S_{or} in the enormous rock is very low.

If we draw saturation against bond number on a log-log scale in the wider range (Fig. 7), we see three different zones as follow, in the first part B is very small and there is not a strong effect and the behavior of the non wetting cluster is the same as in the invasion percolation, in the second part the gravity and the capillarity act simultaneously, and this regime is characterized by the growth of a single branch, so we see a decrease of the saturation by increasing the bond number and in the third section the gravity effect predominates and hides the heterogeneity and the capillary forces; the displacement is then purely vertical and the saturation S is equal to (1/L) and it becomes constant.

In the case of secondary migration, the direction of oil may not always be from the bottom to the top surface, for example there may be a flow movement from the left edge toward the right. Again simulation results in this case shows that by increasing the bond number the finger width decreases and because of a lower density, it goes upward again. Fig. 8 shows some realisations to illustrate this effect.

Then we measure the width of the finger cluster and saturation at different bond number by simulation of 50 samples. The results are shown in figure 9 and 10. These results show that the slops correspond to the width of the finger cluster and saturation is respectively -0.51 and -0.44 which are consistent with theoretical predictions and the results of the previous cases.

These results show that Eqs. (10) and (14) can also be applicable in this case. The numerical results show that in this case the range of bond numbers is wider
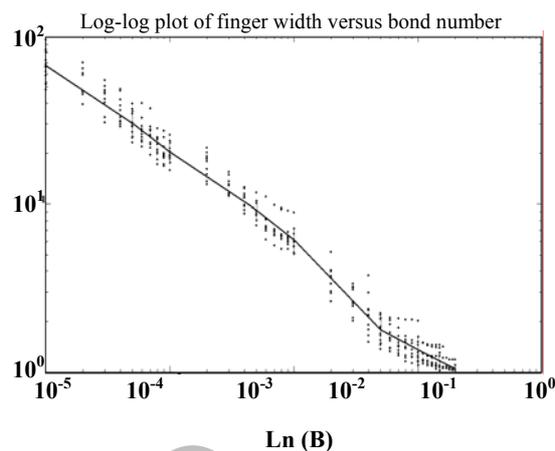

Fig. 5: Variation of width of finger versus bond number on a log-log scale for 10 samples which shows a slope of -0.58.
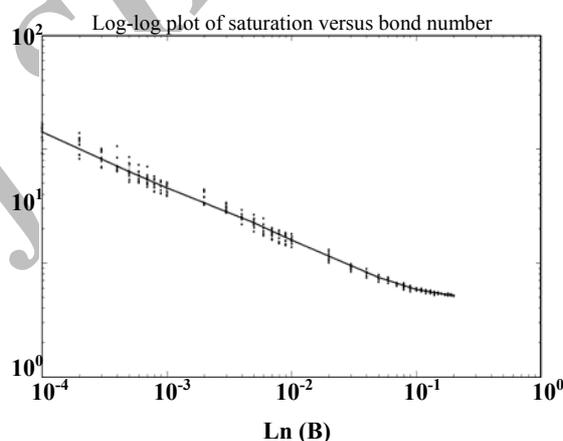

Fig. 6: Variation of saturation versus bond number on a log-log scale for 10 samples which shows a slope of -0.44.
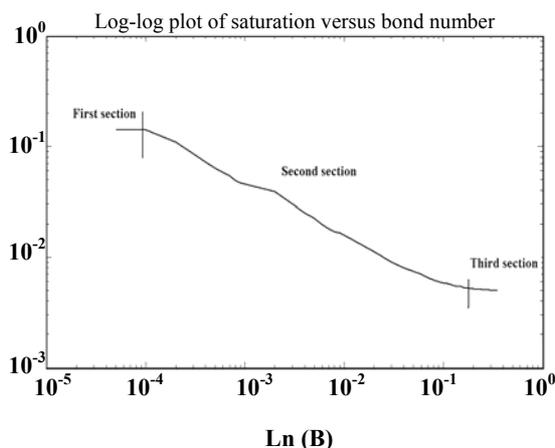

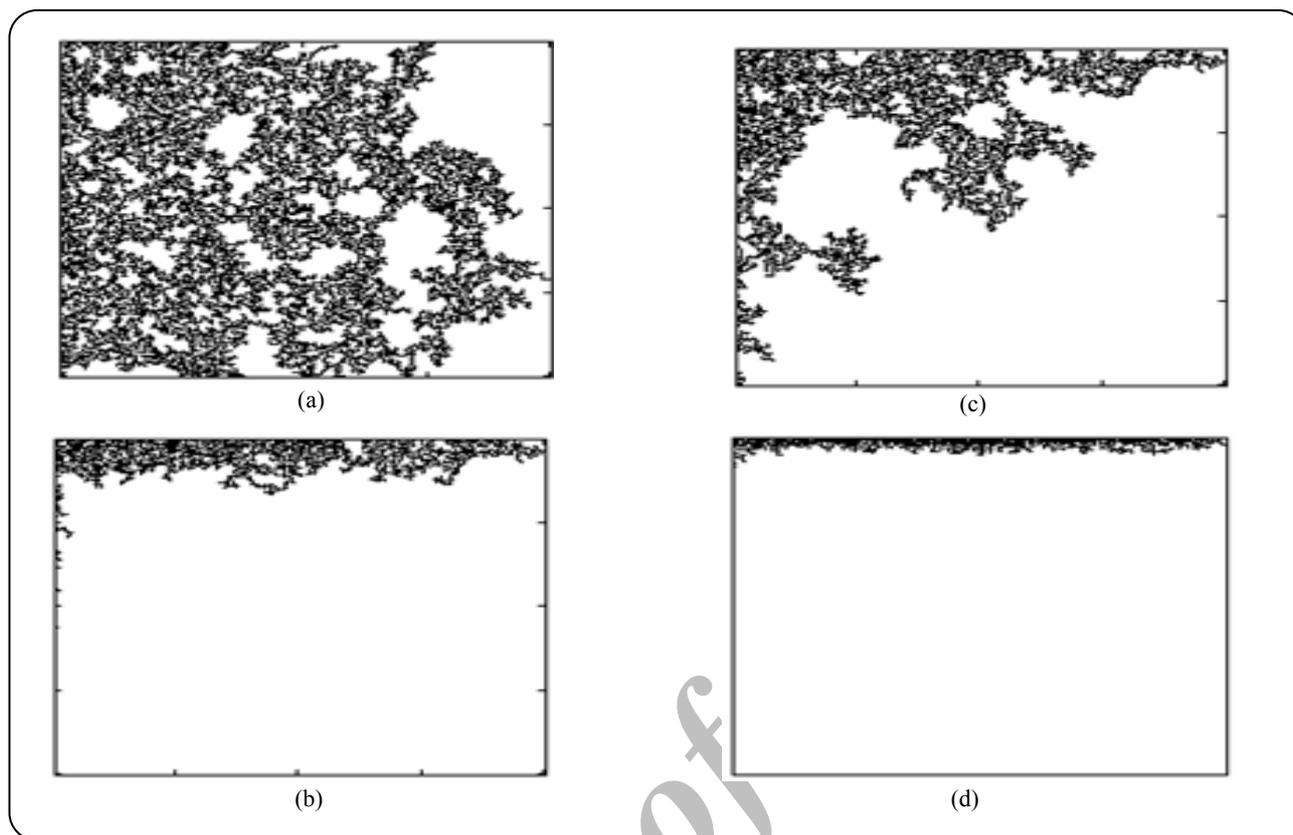**Fig. 7: Three zones for the saturation-bond number variations on a log-log scale.**

Fig. 8 : Four realizations generated by the slow gravity destabilized displacement of a wetting fluid by a non wetting fluid in a quasi-two-dimensional porous medium in a lattice of size 200×200*, when non wetting fluid invade from left side where (a) B=0, (b) B=-0.0001, (c) B=-0.001,(d) B=-0.01.*

(-0.0001 to -0.45) in comparison to the previous condition (-0.0001 to -0.25), therefore the effect of gravity is more sensible in the case of vertical movement of non wetting fluid with respect to its lateral movement and the width of finger cluster; hence, its saturation reaches the lowest value earlier. In Fig. 11 we show these differences in saturation against the bond number; again this can reasonably describe why we see very small residual oil saturation (less than 1%) at the end of secondary migration process.

If we assume that for filling each site we require a time step, then by counting the amount of filling site we can predict the breakthrough for each lattice as follows:

$$\tau \sim N \quad \rightarrow \quad \tau \sim S_0 \qquad (15)$$

Therefore this breakthrough time scales with the bond number as,

$$\tau \sim B^{-\gamma} \qquad (16)$$

NUMERICAL INVESTIGATION OF THE EFFECT OF PORE SIZE DISTRIBUTION ON THE IPG DESTABILIZED PROCESS

In this part we consider a lattice of size 200×200; an invasion fluid (oil) that enters from the left side of the lattice and displaces water (e.g. the process which happens in the secondary migration) on a lattice of different pore size distribution (such as uniform, normal and lognormal distributions) and study the effect of pore size distribution on the network properties. We assume that all conditions are the same and the only difference is in the pore size distribution, then for each pore size distribution we consider 50 samples and calculate the saturation and width of finger of invasion fluid at the breakthrough time in various bond numbers ranges from -0.0001 to -0.4 and calculate the slope of them on a log-log scale (Figs. 12 and 13).

We see that for the saturation results (Fig. 12), the slope of the saturation versus the bond number on a
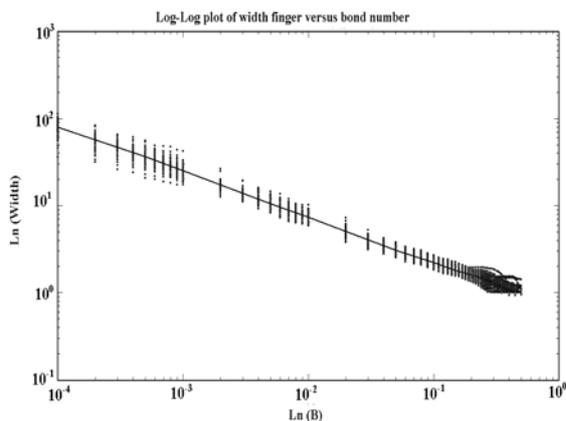
79

Fig. 9: Width of finger against bond number on log-log scale for 50 samples when oil injected from left edge. This shows that the slope is equal to -0.51.
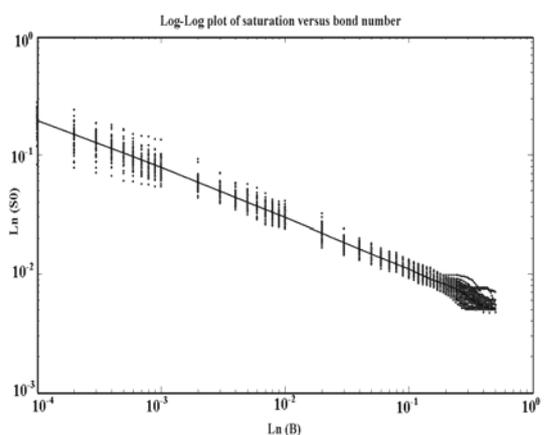

Fig. 10: Saturation against bond number on log-log scale for 50 samples when oil injected from left edge. This shows that the slope is equal to -0.44.
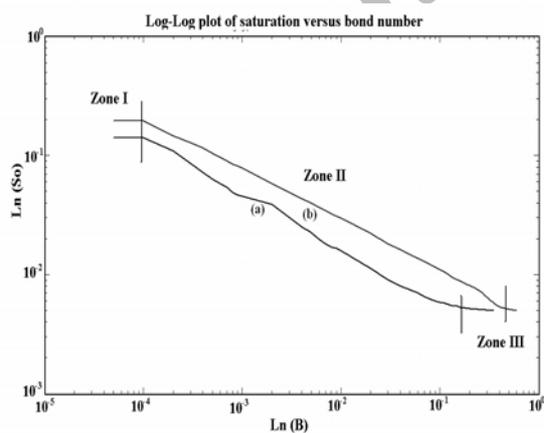

Fig. 11: Comparison of range of bond number in the case of injection of invader fluid from bottom of lattice (a) and in the case of injection of invader fluid from left side of lattice (b).

log-log scale for the uniform, normal and lognormal distribution is -0.4760, -0.4574 and -0.4360 respectively, and for the finger width results (Fig. 13) the slope of the width against the bond number on a log-log scale for the uniform, normal and lognormal distribution is -0.5836, -0.5557 and -0.5193 respectively.

These results demonstrate that it is reasonable to assume that the distribution of the capillary pressure is slowly varying near the percolation threshold p_c. However, in the case of saturation results, the pore size distribution does not affect the exponent observed in the power law scaling greatly. Moreover, the amplitude of S_o is very sensitive to the pore size distribution, implying that the distribution and the magnitude of the capillary forces play important roles in determining the displacement patterns and the saturation at the percolation threshold.

In the next step we consider a composite lattice with pore size distribution in Fig. 14.

Then we calculate the saturation and the finger width as before for 50 samples and study the behaviour of the system under this condition. We calculate the slope of the curves in log-log scale (Fig. 15) and see that this behaviour is different from the previous cases and it has an average slope of -0.3702 for the saturation and -0.4596 for the finger width. One may notice that the decrease in slope of the saturation results, for example, emphasizes the effect of heterogeneity represented by considering the widest pore size distribution to be at bottom and narrower at the top.

CONCLUSIONS

We have described the basis of various displacement processes in porous media and discussed the modeling techniques for them. In particular, we have shown that for the capillary dominated flow regime invasion percolation is an appropriate model to describe the displacement process. In particular, we have shown how the gradient percolation along with simulation results can be used to incorporate the effects of gravity forces in the displacement modeling. Moreover, the width of the finger cluster on the interface of two immiscible phases and the saturation of the invading fluid with respect to the bond number are presented numerically. This result can reasonably describe why we see very small residual oil saturation (less than 1%) at the end of secondary migration process. Moreover, we have shown that the pore size
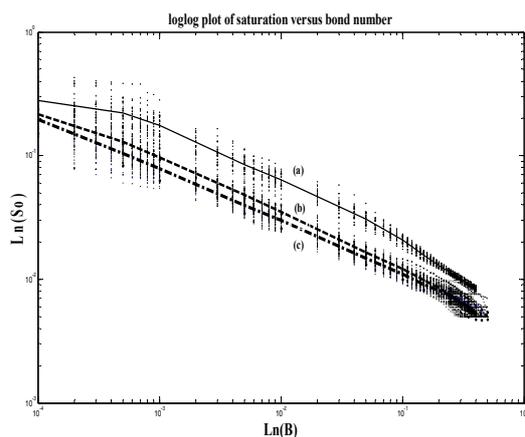
Fig. 12: Comparison of saturation slop respect to bond number on a log-log scale for uniform (solid line (a)), normal (dashed line (b)) and lognormal (dashed dot line(c)) distributions.
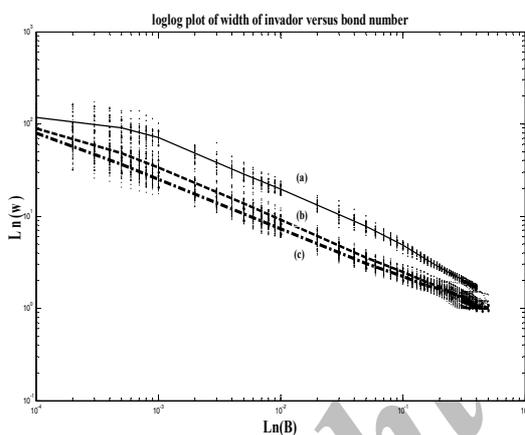

Fig. 13: Comparison of finger width slop respect to bond number on a log-log scale for uniform (solid line(a)), normal (dashed line (b)) and lognormal (dashed dot line(c)) distributions.
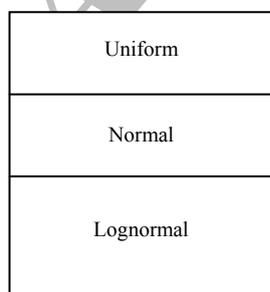

Fig. 14: Arrangement of the pore size distribution in a composite lattice.

distribution as a measure of the system heterogeneity can greatly affect the flow displacement behavior. In particular, it affects the scale dependency of both saturation and the width of the finger cluster by decreasing the exponents of the corresponding power law scaling. This effect is clearer in the case where the widest pore size distribution is at the bottom and the narrower at the top of the system. As a result, this study improves our understanding of the slow displacement of the fluid flow under the presence of gravity in a geometrically complex medium.

Nomenclatures

B_o	Dimensionless Bond number
d	Fractal dimension
g	Acceleration due to gravity
g (r)	Two point correlation function
K	Absolute permeability
k_{ri}	Relative permeability
L	Lattice size
M	Cluster mass
N_I	Number of sites occupied by the invader in spanning cluster
p	Occupancy probability
p_c	Percolation threshold
p_c^∞	Percolation threshold of infinite systems
P_i	Phase pressure
P_{nw}	Pressure of non wetting phase
P_w	Pressure of wetting phase
P_c	Capillary pressure
P(p)	Connected fraction
r	Pore throat radius
S_i	Fluid saturations
t	Time
u_i	Phase velocity
Y(i)	y-coordinate of the ith site
β, ν	Critical exponents
σ	Interfacial tension
$\Delta\rho$	Density difference between the two fluids
θ	Contact angle
ϕ	Porosity
η	Viscosity
ε	Pore or grain characteristic size
ζ	Size of blobs
γ	Exponent for the saturation
τ	Breakthrough time
ξ	Correlation length

81

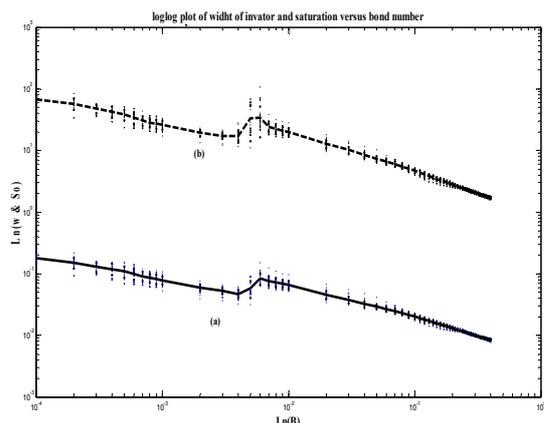**Fig. 15: Saturation (solid line (a)) and finger width (dashed line (b)) respect to bond number on a log-log scale for the composite lattice.**

REFERENCES

[1] Sahimi M, "Flow and Transport in Porous Media and Fractured Rock", VCH Publication (1995).

[2] Wilkinson D, Percolation Model of Immiscible Displacement in the Presence of Buoyancy Forces, *Physical Review A,* **34** (1), p. 520 (1984).

[3] Fatt, I., The Network Model of Porous Media, *Transactions of AIME* 207, p. 144 (1956).

[4] Blunt M., King P. R., Macroscopic Parameters from Simulations of Pore Scale Flow, *Physical Review, A,* **42**(12), p. 4780 (1990).

[5] Bryant S., Blunt M., Prediction of Relative Permeability in Simple Porous Media, *Physical Review A,* **46**, p. 2004 (1992).

[6] Øren, P.E., Bakke, S., Arntzen, O.J., Extending Predictive Capabilities to Network Models, *SPE J.,* **3**, p. 324 (1998).

[7] Piri M., "Pore Scale Modelling of Three Phase Flow, PhD Thesis, Centre for Petroleum Studies, Department of Earth Science and Engineering", Imperial College, London (2003) .

[8] Broadbent S.R, Hammersley J.M., Percolation Processes. 1. Crystals and Mazes. Proc. *Cambridge Phil. Soc.*, **53**, p. 629 (1957).

[9] Stauffer D., Aharony A., "Introduction to Percolation Theory", Taylor and Francis, London (1992).

[10] Sahimi M., "Application of Percolation Theory", VCH Publication (1995).

[11] Wilkinson D., Willemsen J.F., Invasion Percolation: a New form of Percolation theory, *Journal of Physics A: Mathematical and General,* **16**(16), p. 3365 (1983).

[12] Toubou E., Lenormand R. and Zarcon C., Immiscible Displacement in Porous Media: Testing Network Simulators by Micromodel Experiments, Presentation at the 62nd Annual Technical Conference and Exhibition of the Society of Petroleum Engineering (SPE) in Dallas. TX, September 27-30 (1987).

[13] Zhang Y., Shriati M., Yortsos Y.C., The Spreading of Immiscible Fluids in Porous Media under the Influence of Gravity, *Transport in porous media,* **38**, p. 117 (2000).

[14] Masihi M., King P. R., Connectivity Prediction in Fractured Reservoirs with Variable Fracture Size; Analysis and Validation, *SPE Journal,* **13** (1), p. 88 (2007)**.**

[15] Bear J., "Dynamics of Fluids in Porous Media", American Elsevier Publishing Company, New York (1972).

[16] Homsy G. M., Viscous Fingering in Porous Media, *Annual Review of Fluid Mechanics,* **19**, p. 271 (1987).

[17] Chandler R., Koplik J., Lerman K., Willemsen J.F., Capillary Displacement and Percolation in Porous Media, *Journal of Fluid Mechanics,* **119**, p. 249 (1982).

[18] Heiba A. A., Sahimi M., Scriven L. E., Davis H. T., Percolation Theory of Two-Phase Relative Permeability, *SPE Reservoir Engineering*, **7**, p. 123 (1992).

[19] Mani V., Mohanty K. K., Pore-Level Network Modelling of Three-Phase Capillary Pressure and Relative Permeability Curves, *SPE Journal,* **3**, p. 238 (1998).

[20] Meakin P., Wagner G., Vedvik A., Amundsen H., Feder J., Jossang T., Invasion Percolation and Secondary Migration: Experiments and Simulations, *Marine and Petroleum Geology,* **17**, p. 777 (2000).

[21] Bo Z., loggia D., Xiaorong L., Vassueur G., Ping H., Numerical Studies of Gravity Destabilized Percolation in 2D Porous Media, *European Physics Journal B,* **50**, p. 631 (2006).